

Evolution of rotating stars at very low metallicity

Georges Meynet¹, Raphael Hirschi², Sylvia Ekström¹, and André Maeder¹

¹*Observatoire Astronomique de l'Université de Genève, CH-1290 Sauverny, Switzerland*

²*Dept. of Physics and Astronomy, University of Basel, CH-4056 Basel*

Abstract. At very low metallicity, the effects of differential rotation have a more important impact on the evolution of stars than at high metallicity. Rotational mixing leads to the production of great quantities of helium and of primary ¹⁴N by massive stars. Rotation induces important mass loss and allows stars to locally strongly enrich the interstellar medium in CNO elements. Stars formed from interstellar clouds enriched by the winds of fast rotating massive stars would present surface abundances similar to those of C-rich extremely metal-poor stars. C-rich stars can also be formed by mass accretion in a binary system where the primary would be a fast rotating intermediate mass star in the early-AGB phase. Fast rotation may also lead to the formation of collapsars even at very low metallicity and make the most massive stars avoid the pair instability.

1. Shellular rotation at very low metallicity

The evolution of non-rotating extremely metal-poor stars has been described recently by many authors (Weiss et al. 2000; Chieffi & Limongi 2002; Nomoto et al. 2003; Tumlinson, Shull, & Venkatesan 2003; Picardi et al. 2004). Here we shall concentrate on the evolution of rotating stars at very low metallicity, a subject which, up to now, has not been so often discussed in literature (although see Heger & Woosley 2002; Marigo et al. 2003 and the contributions by Ekström, Woosley and Yoon in the present volume).

In the models presented in this paper, the effects of the centrifugal acceleration in the stellar structure equations are accounted for as explained in Kippenhahn and Thomas (1970). The equations describing the transport of the chemical species and angular momentum resulting from meridional circulation and shear turbulence are given in Zahn (1992) and Maeder & Zahn (1998). The expressions for the diffusion coefficients are taken from Talon and Zahn (1997) and Maeder (1997). The effects of rotation on the mass loss rates is taken into account as explained in Maeder and Meynet (2001).

These models have been compared with stellar observations in the Galaxy and the Magellanic Clouds. They are able to account for many observational constraints that non-rotating models cannot fit: they can reproduce surface enrichments (Heger & Langer 2000; Meynet & Maeder 2000), the blue to red supergiant ratios at low metallicity (Maeder & Meynet 2001), the variation with the metallicity of Wolf-Rayet populations and of the number ratios of type Ibc to

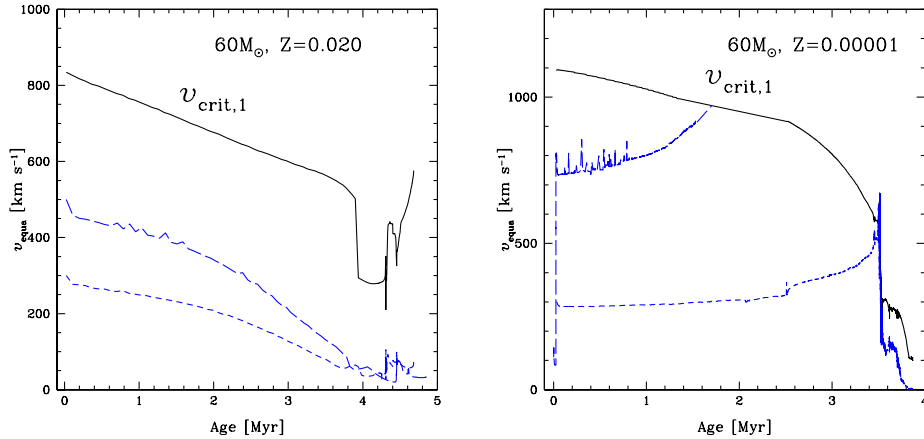


Figure 1. *Left* : Evolution of the surface equatorial velocities at the surface of $60 M_{\odot}$ models at solar metallicity with $v_{\text{ini}} = 300$ (short-dashed line) and 500 km s^{-1} (long-dashed line). The continuous line shows the evolution of the equatorial critical velocity. *Right* : Same as the left part of the figure, for $60 M_{\odot}$ at $Z = 10^{-5}$ with $v_{\text{ini}} = 300$ (short-dashed line) and 800 km s^{-1} (long-dashed line).

type II supernovae (Meynet & Maeder 2004). Having checked that these models compare reasonably well in the metallicity range between $Z=0.004$ and 0.020 , let us now explore what are their predictions for much lower metallicities.

Let us note before, that if the effects of rotation are already quite significant at high metallicity, one expects them to be even more important at lower metallicity. For instance, it was shown in previous works that the chemical mixing becomes more efficient at lower metallicity for a given initial mass and velocity (Maeder & Meynet 2001; Meynet & Maeder 2002). This comes from the fact that the gradients of Ω are much steeper in the lower metallicity models, so they trigger more efficient shear mixing. The gradients are steeper because less angular momentum is transported outwards by meridional currents, whose velocity scales as the inverse of the density in the outer layers (see the Gratton-Öpik term in the expression for the meridional velocity in Maeder & Zahn 1998). An interesting consequence of this greater mixing efficiency is the possibility for metal-poor rotating stars to produce important amounts of primary nitrogen (Meynet & Maeder 2002).

1.1. The case of massive stars

In very metal-poor massive stars, rotation can trigger important mass loss in many ways. The first way, paradoxically, is linked to the fact that very metal-poor stars are believed to lose little mass by radiatively driven stellar winds. Since metal-poor stars lose little mass, they also lose little angular momentum (if rotating), so they have a greater chance of reaching the break-up limit during the Main Sequence phase. At break-up, the outer stellar layers become unbound and are ejected whatever their metallicity. The break-up is reached more easily when the wind anisotropy induced by rotation are taken into account (Maeder 1999).

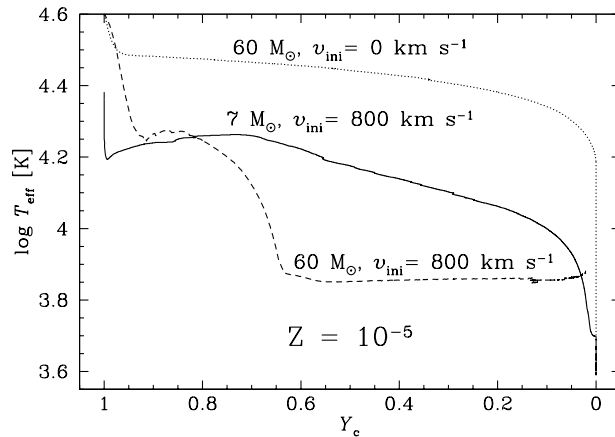


Figure 2. Evolution of $\log T_{\text{eff}}$ as a function of Y_c , the mass fraction of ${}^4\text{He}$ at the centre, for a non-rotating (dotted line) and rotating (dashed line) $60 M_{\odot}$ model at $Z = 10^{-5}$. The continuous line show the case of a $7 M_{\odot}$ stellar model.

In Fig. 1, the evolution of the surface velocity for $60 M_{\odot}$ stellar models at two different metallicities is shown. We see that at solar metallicity, the mass loss rates are so high that, even starting with an initial velocity of 500 km s^{-1} , the star does not reach the critical limit. As explained above, the situation is quite different at lower Z , due to the metallicity dependence of the mass loss rates: for the metallicity range between 10^{-4} and $1 \times Z_{\odot}$, Kudritzki (2002) obtains $\dot{M}(Z) \propto (Z/Z_{\odot})^{0.5} \dot{M}(Z_{\odot})$. Starting with $v_{\text{ini}} = 300 \text{ km s}^{-1}$, the star reaches the critical limit at the end of the Main-Sequence phase. With an initial velocity of 800 km s^{-1} the critical limit is reached at a much earlier time.

Another way for rotation to trigger enhancements of the mass loss comes from the mixing induced by rotation. In general, rotational mixing favours the evolution into the red supergiant stage (see Maeder & Meynet 2001), where mass loss is higher. This is illustrated in Fig. 2. One sees that the $60 M_{\odot}$ non-rotating model remains on the blue side during the whole core He-burning phase, while the 800 km s^{-1} model at $Z = 10^{-5}$ starts its journey toward the red side of the HR diagram early in the core helium burning stage, when $Y_c \simeq 0.67$ (Y_c is the mass fraction of helium at the centre of the stellar model). The same is true for the corresponding model at $Z = 10^{-8}$. Let us recall that this behaviour is linked to the rapid disappearance of the intermediate convective zone associated to the H-burning shell.

Rotational mixing also enhances the metallicity of the surface of the star and, in this way, may boost radiatively driven stellar winds. Figure 3 shows the evolution as a function of the remaining mass of the abundances at the surface of a rotating $60 M_{\odot}$ stellar model at $Z=10^{-5}$ with $v_{\text{ini}}= 800 \text{ km s}^{-1}$. During a first phase, the actual mass decreases from 60 to about $51 M_{\odot}$, and the surface metallicity (here defined as the sum of the mass fractions of all the elements except hydrogen and helium) remains equal to the initial one. The changes of the surface abundances are due to rotational mixing and reflect the arrival at the surface of CNO processed material (decrease of ${}^{12}\text{C}$ and ${}^{16}\text{O}$ abundances and increase of ${}^{14}\text{N}$ abundance, while the sum of CNO elements remains constant).

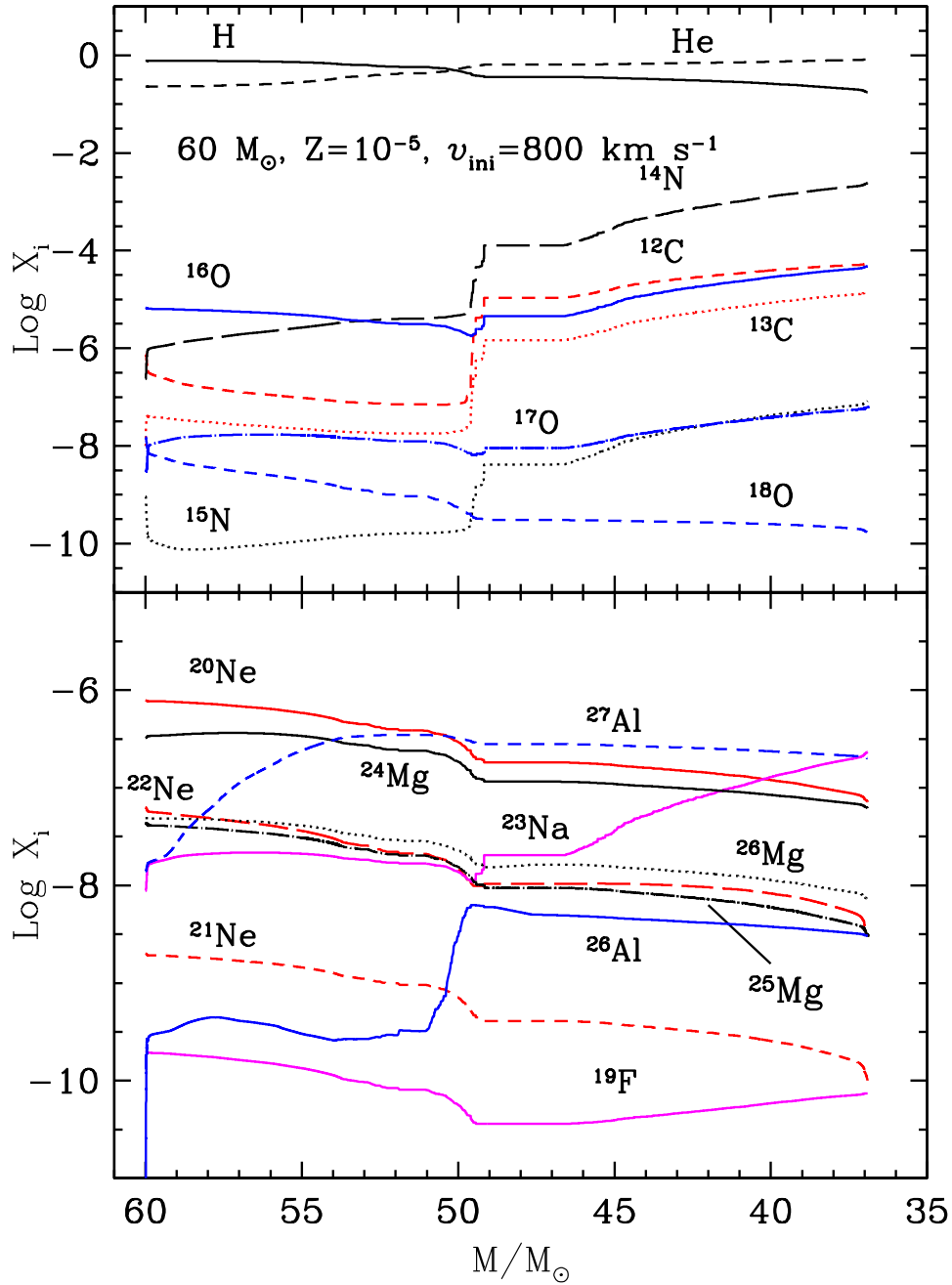


Figure 3. Evolution as a function of the remaining mass of the surface abundances in mass fraction of various elements for a $60 M_\odot$ stellar model at $Z = 10^{-5}$ and with $v_{\text{ini}} = 800 \text{ km s}^{-1}$.

The mass lost during this phase (about $9 M_\odot$) results from radiatively driven stellar winds and evolution at the break-up limit.

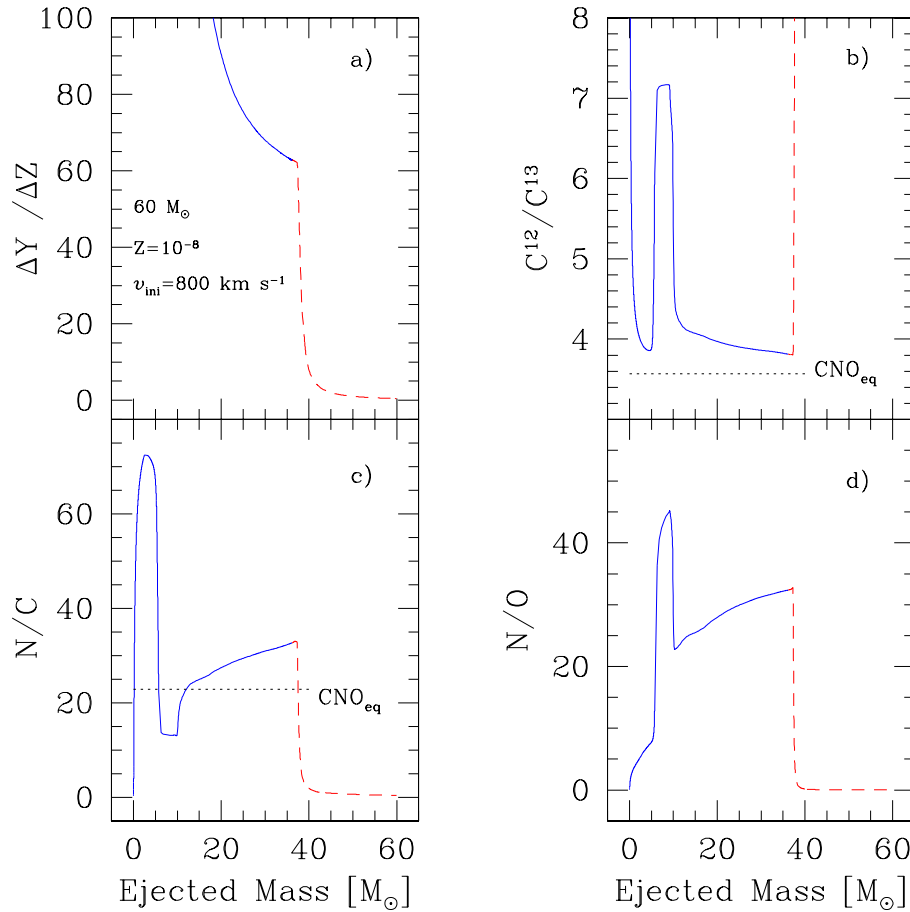


Figure 4. Variation as a function of the ejected mass of: **a)** the ratio of the newly synthesized helium ΔY to the newly synthesized heavy elements ΔZ in the ejecta; **b)** the ratio of $^{12}\text{C}/^{13}\text{C}$; **c)** the ratio of nitrogen to carbon; **d)** the ratio of nitrogen to oxygen. The case for a rotating $60 M_{\odot}$ model at $Z=10^{-8}$ is shown. The continuous line corresponds to the mass ejected by stellar winds, the dashed line shows how the ratios vary when the mass from the presupernova model is added. The dotted lines indicate the ratios obtained in the convective core of the star, when the mass fraction of hydrogen at the centre is 0.34. They correspond to CNO equilibrium values. The corresponding CNO equilibrium value for the N/O ratio is 152.

When the actual mass is around $51 M_{\odot}$, the star is at the middle of the core He-burning phase (Y_c equal to 0.45) and with $\log T_{\text{eff}}=3.850$. From this stage on, an outer convective zone deepens in mass, dredging-up material to the surface. This produces the sharp increase in the surface abundances in ^{12}C , ^{13}C , ^{14}N , and ^{15}N . Then, the total amounts of heavy elements increases up to a value corresponding to more than 240 times the initial heavy element mass fraction. As can be seen from Fig. 3, the wind is strongly enriched in carbon, nitrogen, sodium and aluminium and also, to a less extent, in oxygen.

It is interesting to look at the way the ratios $\Delta Y/\Delta Z$ (mass fraction of newly synthesized helium ΔY to the mass fraction of newly synthesized heavy elements ΔZ), $^{12}\text{C}/^{13}\text{C}$, N/C and N/O (in mass fraction) vary as a function of the mass ejected in the wind during the stellar lifetime. This is shown in Fig. 4 for the case of the $60 M_{\odot}$ stellar model at $Z = 10^{-8}$ with $v_{\text{ini}} = 800 \text{ km s}^{-1}$. At the beginning $\Delta Y/\Delta Z$ is not defined, it would be equal to $0/0$. Then it tends to infinity when some newly synthesized helium appears at the surface, while no new heavy elements have yet reached the surface. When the ejected mass approaches about $18 M_{\odot}$, $\Delta Y/\Delta Z \sim 100$, and at the end of the stellar lifetime $\Delta Y/\Delta Z \sim 65$ in the wind ejecta. The new heavy elements at this stages are in the form of new CNO elements. No newly synthesized iron is ejected in the winds.

The initial ratios for $^{12}\text{C}/^{13}\text{C}$, N/C and N/O are respectively 75.5, 0.31 and 0.03. The variations of the $^{12}\text{C}/^{13}\text{C}$ and N/C ratios are quite rapid (see Fig. 4). Both ratios change by more than an order of magnitude in the wind ejecta, when only $6 M_{\odot}$ are lost. As expected from nuclear physics, at the beginning, the variation of the N/O ratio is relatively slow, then, the ratio varies in a very short timescale by more than two orders of magnitude.

When about $6 M_{\odot}$ have been lost, the star encounters the Humphreys-Davidson limit and loses in a short while about $4\text{-}5 M_{\odot}$ of its H-rich envelope. No big changes of the N/C and N/O ratios are seen, the $^{12}\text{C}/^{13}\text{C}$ increases by a little less than a factor 2.

The last phase, which is also the one during which the greatest amount of mass is lost, begins when about $10 M_{\odot}$ have been ejected. During this phase primary nitrogen, accompanied by carbon and oxygen synthesized in the He-burning core, arrives at the surface. On average, values of $^{12}\text{C}/^{13}\text{C}$ equal to about 4 are obtained, while the N/C and N/O ratios have values of about 30.

The dashed line in Fig. 4 shows how the addition of material from the presupernova model changes the ratios. When the supernova ejecta are taken into account, much lower values of $\Delta Y/\Delta Z$, N/C and N/O are obtained, and much higher $^{12}\text{C}/^{13}\text{C}$ ratios. The addition of a very small amount of mass ejected by the supernova already changes a lot the ratios. For instance, the addition of only $4 M_{\odot}$ ejected at the time of the supernova explosion would lower the N/C ratio from the value of 33 to about 2.

The importance of the various enrichments depends on metallicity, the initial mass and the initial velocity considered. The case of the $85 M_{\odot}$ models at $Z = 10^{-8}$, with $v_{\text{ini}} = 800 \text{ km s}^{-1}$ is shown in Fig. 5 (Hirschi 2005). This model loses more than 75% of its initial mass, and will terminate its life as a WO star. Interestingly, its angular momentum content at the presupernova stage is sufficient for giving birth to a collapsar (see also Hirschi, Meynet & Maeder 2005) now considered as among the best candidates for the progenitors of Gamma Ray Bursts (see Woosley 1993; Mazzali et al. 2003). Therefore, according to such models (without magnetic fields), GRB may be produced even at very low metallicity.

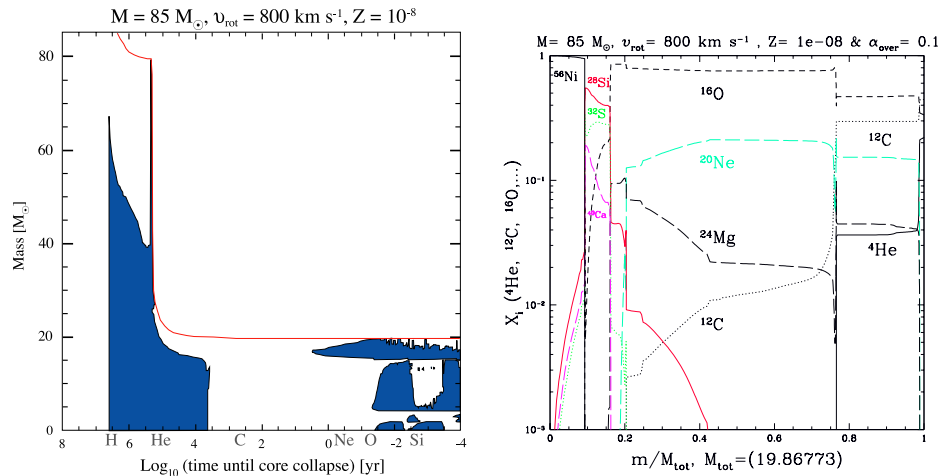


Figure 5. *Left* : Evolution of the total mass for a rotating $85 M_{\odot}$ stellar model as a function of the logarithm of the time before the supernova explosion. The dark areas correspond to convective zones. *Right* : Variation of the chemical composition as a function of the lagrangian mass normalised to the total actual mass at the end of the core Si-burning stage for the same model as in the left part of the figure. Both figures are from Hirshi (2005).

1.2. Do massive very metal-poor, stars end their lives as pair-instability supernovae?

Might the important mass loss undergone by rotating models prevent the most massive stars from going through pair instability? According to Heger & Woosley (2002), progenitors of pair-instability supernovae have helium core masses between ~ 64 and $133 M_{\odot}$. This corresponds to initial masses between about 140 and $260 M_{\odot}$. Thus the question is whether stars with initial masses above $140 M_{\odot}$ can lose a sufficient amount of mass to have a helium core that is less than about $64 M_{\odot}$ at the end of the core He-burning phase. From the values quoted above, it would imply the loss of more than $(140-64) M_{\odot} = 76 M_{\odot}$, which represents about 54% of the initial stellar mass. From the computations presented here, where a $85 M_{\odot}$ loses more than 75% of its initial mass, one can expect that such a scenario is possible. However, more extensive computations are needed to check in which metallicity range and for which initial velocities rotational mass loss could indeed prevent the most massive stars from going through pair instability. Let us note that, for the same initial velocities as considered here, Pop III stellar models would not avoid the pair instability (see the contribution by Ekström et al. in this volume), however the results might be different for higher initial velocities.

Would pair instability be avoided, this would explain why the nucleosynthetic signature of pair-instability supernovae is not observed in the abundance pattern of the most metal-poor halo stars known up to now. At least this rotational mass loss could restrain the mass range for the progenitors of pair-instability supernovae, pushing the minimum initial mass needed for such a scenario to occur to higher values. Moreover, when the initial mass increases, the luminosity of the star comes nearer to the Eddington limit. When rotating,

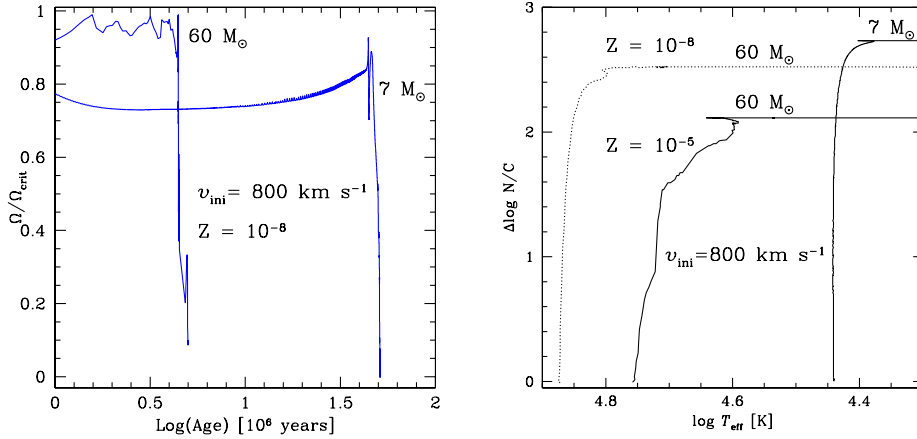


Figure 6. *Left:* Evolutions of the ratio of the actual angular velocity to the critical angular velocity at the surface of a rotating 60 and $7 M_{\odot}$ stellar model at very low metallicity. *Right:* Evolution as a function of the effective temperature of the N/C ratio ($\Delta \log N/C = \log(N/C) - \log(N/C)_{\text{ini}}$) at the surface of the two same models. The dotted line corresponds to a $60 M_{\odot}$ stellar model at $Z = 10^{-8}$ with the same initial velocity.

such stars will then encounter the $\Omega\Gamma$ -limit (Maeder & Meynet 2001) and very likely undergo strong mass losses.

1.3. The intermediate mass stars

Rotation not only affects the evolution of massive stars but also that of intermediate mass stars. In Fig. 6, the evolution of the equatorial velocity and of the nitrogen to carbon ratio at the surface of a $7 M_{\odot}$ stellar model is shown. They are compared to the evolution of the corresponding quantities in $60 M_{\odot}$ models. While the $60 M_{\odot}$ model rapidly reaches the break-up limit, the $7 M_{\odot}$ maintains during most of the Main-Sequence phase a value of $\Omega/\Omega_{\text{crit}}$ equal to 0.8 at the surface. Let us note that the outer layers of the $7 M_{\odot}$ stellar model are denser than in more massive stellar models. Thus, the Gratton-Öpik term ($\propto 1/\rho$) in the expression of the meridional velocity is therefore smaller, making the outwards transport of the angular momentum less efficient. In the $7 M_{\odot}$ stellar model, the gradients of Ω are steeper and the chemical mixing is thus more efficient. This can be seen in the right part of Fig. 6.

2. Links with the C-rich extremely metal-poor stars

If most stars at a given $[\text{Fe}/\text{H}]$ present great homogeneity in composition, a small group, comprising about 20 - 25% of the stars with $[\text{Fe}/\text{H}]$ below -2.5 , show very large enrichments in carbon. These stars are known as C-rich extremely metal-poor (CEMP) stars. The observed $[\text{C}/\text{Fe}]$ ratios are between ~ 2 and 4, showing a large scatter. Other elements, such as nitrogen and oxygen (at least in the few cases where the abundance of this element could be measured), are also highly enhanced. Interestingly, the two most metal-poor stars known up to now, the

Christlieb star (HE 0107-5240), a halo giant with $[\text{Fe}/\text{H}]=-5.3$ (Christlieb et al. 2004), and the subgiant or main-sequence star HE 1327-2326 with $[\text{Fe}/\text{H}]=-5.4$ (Frebel et al. 2005) belong to this category.

A few CEMP stars are Main-Sequence or subgiant stars like the Frebel star. At these evolutionary stages, no process occurring in the star itself can explain the surface abundances. For these stars at least, the surface abundances reflect the abundances of the protostellar cloud from which the star formed, or the surface abundances of a more evolved companion whose part of the mass has been accreted by the CEMP star.

To explain the very high C-abundance, various models have been proposed. For instance, Umeda & Nomoto (2003) propose that the cloud from which HE 0107-5240 formed was enriched by the ejecta of one Pop III 25 M_{\odot} star, which had exploded with low explosion energy (on the order of 3×10^{50} erg) and experienced strong mixing and fallback at the time of the supernova explosion. This would mimic asymmetric explosions. Limongi & Chieffi (2003) suggest that the cloud was enriched by the ejecta of two Pop III supernovae from progenitors with masses of about 15 and 35 M_{\odot} . Some authors have proposed that this particular abundance pattern results from accretion of interstellar material and from a companion (for instance an AGB star, as proposed by Suda et al. 2004).

Recently, we have explored the possibility that such CEMP stars could be formed from the wind ejecta of massive rotating stars (Meynet et al. 2005). Let us suppose that these massive stars produce, at the end of their nuclear lifetime, a black hole, that swallows the whole final mass. In that case, the massive star would contribute to the local chemical enrichment of the interstellar medium only through its winds. In Fig. 7 the abundances in the winds of various initial mass models are plotted (Hirschi 2005). We see that for all masses superior to about 40 M_{\odot} enhancements of CNO elements with respect to iron are obtained. For comparison the enhancements of these elements observed at the surface of CEMP stars are indicated by hatched areas. The continuous line corresponds to the abundance in pure wind material. When the wind material of the 40 M_{\odot} stellar model is mixed with hundred times more of interstellar material, the dot-dashed curve is obtained. We see that wind material, diluted with some interstellar matter, could reproduce the CNO abundance pattern observed at the surface of CEMP stars.

What does happen now if the supernova also contributes to the enrichment of the cloud ? From the mass of CO-core M_{CO} it is possible to infer the mass of the remnant M_{rem} using the relation of Arnett (1991) between M_{CO} and M_{rem} . The value M_{rem} obtained is equal to 5.56 M_{\odot} for the 60 M_{\odot} stellar model shown in Fig. 4. In Fig. 4, this corresponds to a total mass ejected of 54.44 M_{\odot} (60-5.56). The values of $\Delta Y/\Delta Z$, $^{12}\text{C}/^{13}\text{C}$, N/C and N/O in the ejecta are then respectively 0.68, 309, 0.5 and 0.02. These values are not compatible with the ratios observed at the surface of CS 22949-037 (Depagne et al. 2002): $^{12}\text{C}/^{13}\text{C} \sim 4$, N/C ~ 3 and N/O ~ 0.2 . To obtain a better fit in the frame of such models, much less mass from the presupernova should be ejected, confirming the idea of strong fallback proposed by Umeda & Nomoto (2003).

The physical conditions encountered in the advanced phases of an intermediate mass star are not so different from the one realised in massive stars. Thus the same nuclear reaction chains can occur and lead to similar nucleosynthetic

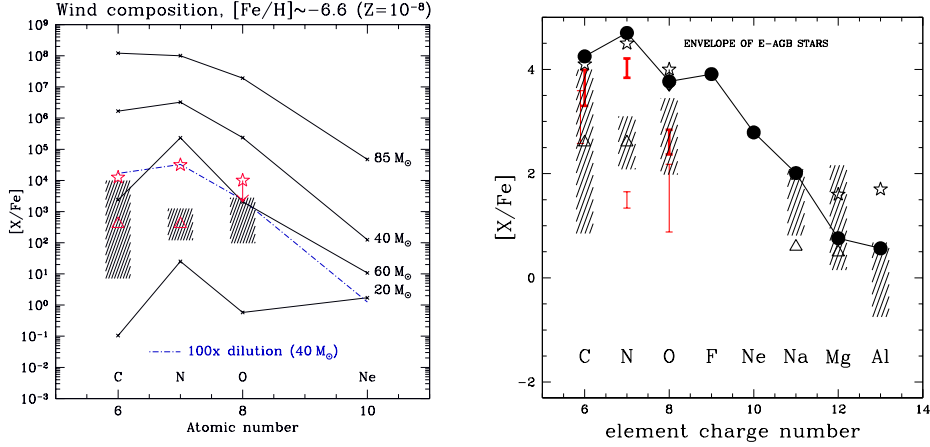


Figure 7. *Left* : Chemical composition of the wind of rotating models (continuous lines) of various initial masses from the work of Hirschi (2005). When the wind material of the 40 M_{\odot} stellar model is mixed with hundred times more of interstellar material, the dot-dashed curve is obtained. The hatched areas correspond to the range of values measured at the surface of giant CEMP stars: HE 0107-5240, $[\text{Fe}/\text{H}] \simeq -5.3$ (6); CS 22949-037, $[\text{Fe}/\text{H}] \simeq -4.0$ (Norris et al. 2001; Depagne et al. 2002); CS 29498-043, $[\text{Fe}/\text{H}] \simeq -3.5$ (2). The empty triangles (Plez & Cohen 2005, $[\text{Fe}/\text{H}] \simeq -4.0$) and stars (Frebel et al. 2005, $[\text{Fe}/\text{H}] \simeq -5.4$, only an upper limit is given for $[\text{O}/\text{Fe}]$) correspond to non-evolved CEMP stars (see text). *Right* : Chemical composition of the envelopes of E-AGB stars compared to abundances observed at the surface of CEMP stars (references as in the left part of the figure). The continuous line shows the case of a 7 M_{\odot} at $Z = 10^{-5}$ ($[\text{Fe}/\text{H}] = -3.6$) with $v_{\text{ini}} = 800 \text{ km s}^{-1}$. The vertical lines (shown as “error bars”) indicate the ranges of values for CNO elements in the stellar models of Meynet & Maeder (2002) (models with initial masses between 2 and 7 M_{\odot} at $Z = 10^{-5}$). The thick and thin “error bars” correspond to rotating ($v_{\text{ini}} = 300 \text{ km s}^{-1}$) and non-rotating models.

products. Also the lifetimes of massive stars (on the order of a few million years) are not very different from the lifetimes of the most massive intermediate mass stars; typically a 7 M_{\odot} has a lifetime on the order of 40 Myr, only an order of magnitude higher than a 60 M_{\odot} star. Moreover, the observation of s-process element overabundances at the surface of some CEMP stars also point toward a possible Asymptotic Giant Branch (AGB) star origin.

To explore a scenario where the particular surface abundances of the CEMP star results from a mass transfer from a primary in the AGB stage, Meynet et al. (2005) computed a 7 M_{\odot} with $v_{\text{ini}} = 800 \text{ km s}^{-1}$ at $Z = 10^{-5}$. In contrast to the 60 M_{\odot} models, the 7 M_{\odot} stellar model loses little mass during the core H- and He-burning phase, so that the star has still nearly its whole original mass at the early asymptotic giant branch stage (the actual mass at this stage is 6.988 M_{\odot}). This is because the star never reaches the break-up limit during the MS phase (see Fig. 6). Also, due to rotational mixing and dredge-up, the metallicity enhancement at the surface only occurs very late, when the star evolves toward the red part of the HR diagram after the end of the core He-burning phase. At

this stage, the outer envelope of the star is enriched in primary CNO elements, and the surface metallicity reaches about 1000 times the initial metallicity. If such a star is in a close binary system, there is a good chance that mass transfer occurs during this phase of expansion of the outer layers. In that case, the secondary may accrete part of the envelope of the E-AGB star.

From the $7 M_{\odot}$ stellar model, we can estimate the chemical composition of the envelope at the beginning of the thermal pulse AGB phase. Here we call envelope all the material above the CO-core. The result is shown in Fig. 7 (continuous line with solid circles). We also plotted the values obtained from the models of Meynet & Maeder (2002) for initial masses between 2 and $7 M_{\odot}$ at $Z = 10^{-5}$ and with $v_{\text{ini}} = 0$ and 300 km s^{-1} .

We see that the envelopes of AGB stellar models with rotation show a chemical composition very similar to the one observed at the surface of CEMP stars. It is, however, still difficult to say that rotating intermediate mass star models are better than rotating massive star models in this respect. Probably, some CEMP stars are formed from massive star ejecta and others from AGB star envelopes. Interestingly at this stage, some possible ways to distinguish between massive star wind material and AGB envelopes do appear. Indeed, we just saw above that massive star wind material is characterized by a very low $^{12}\text{C}/^{13}\text{C}$ ratio, while intermediate mass stars seem to present higher values for this ratio. The AGB envelopes would also present very high overabundances of ^{17}O , ^{18}O , ^{19}F , and ^{22}Ne , while wind of massive rotating stars present a weaker overabundance of ^{17}O and depletion of ^{18}O and ^{19}F (Meynet et al. 2005). As discussed in Frebel et al. (2005), the ratio of heavy elements, such as the strontium-to-barium ratio, can also give clues to the origin of the material from which the star formed. In the case of HE 1327-2326, Frebel et al. (2005) give a lower limit of $[\text{Sr}/\text{Ba}] > -0.4$, which suggests that strontium was not produced in the main s-process occurring in AGB stars, thus leaving the massive star hypothesis as the best option, in agreement with the result from $^{12}\text{C}/^{13}\text{C}$ in G77-61 (Plez & Cohen 2005) and CS 22949-037 (Depagne et al. 2002).

3. Helium enrichment by the first stellar generations

The question of the enrichment in newly synthesized helium by the first stellar generations was already asked long ago by Hoyle & Tayler (1964). The recent finding of a double sequence in the globular cluster ω Centauri by Anderson (1997) (see also Bedin et al. 2004) and the further interpretation of the bluer sequence by a strong excess of helium requires some reexamination of this very interesting question. The bluer sequence, with a metallicity $[\text{Fe}/\text{H}] = -1.2$ or $Z = 2 \cdot 10^{-3}$, implies a helium content $Y = 0.38$, i.e. a helium enrichment $\Delta Y = 0.14$, which in turn demands a relative helium to metal enrichment $\Delta Y/\Delta Z$ of the order of 70 (Piotto et al. 2005). This value of $\Delta Y/\Delta Z$ is enormous and more than one order of magnitude larger than the current value of $\Delta Y/\Delta Z = 4 - 5$ (Pagel 1992) obtained from observations of extragalactic HII regions. This low value of $\Delta Y/\Delta Z$ is also consistent with the chemical yields from supernovae forming black holes above about $20-25 M_{\odot}$ (Maeder 1992).

Fast rotating massive stars at very low metallicity eject important amounts of material rich in newly synthesized helium. As a numerical example, for the

rotating $60 M_{\odot}$ at $Z = 10^{-8}$, 22% of the initial mass is ejected in the form of newly synthesised helium by stellar winds. From Fig. 4, one also sees that the value of $\Delta Y/\Delta Z$ is equal to about 65 in the wind material. This shows that this type of model do appear as very promising for reexamining the question of the helium enrichment by massive stars at very low Z .

References

- Anderson, J. 1997, Ph. D. thesis, Univ. California, Berkeley.
- Aoki, W., Norris, J.E., Ryan, S.G. et al. 2004, ApJ, 608, 971
- Arnett, D. 1991, in "Frontiers of Stellar Evolution", ed. D.A. Lambert, ASP Conf. Ser., 20, p.385
- Bedin, L., G. Piotto, J. Anderson et al. 2004, ApJ, 605, L128
- Chieffi, A., & Limongi, M. 2002, ApJ, 577, 281
- Christlieb, N., Gustafsson, B., Korn, A.J. et al. 2004, ApJ, 603, 708
- Depagne, E., Hill, V., Spite, M. et al. 2002, A&A, 390, 187
- Frebel, A., Aoki, W., Christlieb, N. et al. 2005, Nature, 434, 871
- Heger, A., & Langer, N. 2000, ApJ, 544, 1016
- Heger, A., & Woosley, S. E. 2002, ApJ, 567, 532
- Hirschi, R. 2005, in preparation
- Hirschi, R., Meynet, G., Maeder, A. 2005, A&A, in press (astro-ph/0507343)
- Hoyle, F., Tayler, R.J. 1964, Nature, 203, 1108
- Kippenhahn, R., Thomas, H.C. 1970, in *Stellar Rotation*, IAU Coll. 4, Ed. A. Slettebak, p. 20
- Kudritzki, R.P. 2002, ApJ, 577, 389
- Limongi, M., Chieffi, A., Bonifacio, P. 2003, ApJ, 594, L123
- Maeder, A. 1992, A&A, 264, 105
- Maeder A. 1997, A&A, 321, 134
- Maeder, A. 1999, A&A, 347, 185
- Maeder, A., Meynet, G. 2001, A&A, 373, 555
- Maeder, A., & Meynet, G. 2001, A&A, 373, 555, (Paper VII)
- Maeder A., Zahn J.P. 1998, A&A 334, 1000
- Marigo, P., Girardi, L., & Chiosi, C. 2003, A&A, 403, 225
- Mazzali, P.A. et al. 2003, ApJ, 599, 95
- Meynet, G., & Maeder, A. 2000, A&A, 361, 101, (Paper V)
- Meynet, G., & Maeder, A. 2002, A&A, 390, 561, (Paper VIII)
- Meynet, G., & Maeder, A. 2004, A&A, in press, (Paper XI)
- Meynet, G., Ekström, S., Maeder, A. 2005, A&A, in press (astro-ph/0510560)
- Nomoto, K., Maeda, K., Umeda, H., Tominaga, N., Ohkubo, T., Deng, J., & Mazzali, P. A. 2003, Memorie della Societa Astronomica Italiana, v.75, p.312
- Norris, J.E. 2004, ApJ, 612, L25
- Norris, J.E., Ryan, S.G., Beers, T.C. 2001, ApJ, 561, 1034
- Pagel, B.E.J., Simonson, E.A., Terlevich, R.J., Edmunds, M.G. 1992, MNRAS 255, 325
- Picardi, I., Chieffi, A., Limongi, M., Pisanti, O., Miele, G., Mangano, G., & Imbriani, G. 2004, ApJ, 609, 1035
- Piotto, G., Villanova, S., Bedin, L.R. et al. 2005, ApJ, 621, 777
- Plez, B., Cohen, J.G. 2005, A&A, 434, 111
- Suda, T., Aikawa, M., Machida, M.N., Fujimoto, M.Y., Iben, I. 2004, ApJ, 611, 476
- Talon, S., Zahn, J.P. 1997, A&A, 317, 749
- Tumlinson, J., Shull & J.M., Venkatesan, A. 2003, ApJ, 584, 608
- Umeda, H., Nomoto, K. 2003, Nature, 412, 793
- Weiss, A., Cassisi, S., Schlattl, H., & Salaris, M. 2000, ApJ, 533, 413
- Woosley, S.E. 1993, ApJ, 405, 273
- Zahn, J.P. 1992, A&A, 265, 115